Research Article

Journal of PeptideScience

Received: 13 October 2014 Revised: 21 January 2015 Accepted: 4 March 2015 Published online in Wiley Online Library: 8 April 2015

(wileyonlinelibrary.com) DOI 10.1002/psc.2776

Adsorption of chemically synthesized mussel adhesive peptide sequences containing DOPA on stainless steel

Neha Chandrasekaran,[a] Simone Dimartino,[a,b] Tejraj Janmale,[c] Steven P. Gieseg[c,d] and Conan J. Fee[a,b]*

The adsorption of proteins at solid–liquid interfaces is important in biosensor and biomaterial applications. Marine mussels affix themselves to surfaces using a highly cross-linked, protein-based adhesive containing a high proportion of *L*-3,4-dihydroxyphenylalanine (DOPA) residues. In this work, the effect of DOPA residues on protein adhesion on stainless steel surfaces was studied using a quartz crystal microbalance with dissipation system. The adsorption of two repetitive peptide motifs, KGYKYYGGSS and KGYKYY, from the mussel *Mytilus edulis* foot protein 5 on stainless steel was studied before and after chemo-enzymatic modification of tyrosine residues to DOPA using mushroom tyrosinase. Conversion from tyrosine to DOPA, evaluated by HPLC, was in the range 70–99%. DOPA-modified sequences showed fourfold greater adhesion than unmodified *M. edulis* foot protein 5 motifs. Copyright © 2015 European Peptide Society and John Wiley & Sons, Ltd.

Keywords: adhesive peptides; DOPA, stainless steel; QCM-D, mushroom tyrosinase

Introduction

Nature has been developing adhesives for millions of years. There are many examples of natural adhesives, such as the glue produced by large kelps that cling to rocky shorelines [1] and plant adhesives for self-healing and protection against defects in wood [2,3]. Some animals produce sticky compounds to defend themselves against predators, while others use them to hunt their prey [4,5].

The earliest reported uses of adhesives by man were to caulk ships with tars for watertightness and to seal jars of spices with asphalt [6]. The industrial development of adhesives first occurred in the 15th century with the increased production of paper and associated use of natural glues. Naturally available adhesives widely exploited for technical applications include casein-based glues derived from milk, latex rubber, and tree gum [7]. Although natural adhesives remain important, modern adhesives in the 20th century have involved the development of synthetic polymers [6].

Biomimetic adhesives are synthetic adhesives designed to mimic the characteristics of adhesives sourced from biological species. The key objective when creating biomimetic adhesives is to replicate the original interactions between the adhesive material and a surface, whether the surface is of biological or non-biological origin [8] and can be based not only on structural features but on specific functions exhibited by natural organisms, such as the extremely strong, multi-surface, and water-resistant adhesion capabilities of mussels. The common blue mussel (*Mytilus edulis*) is emerging as an effective model organism for studying biological adhesion to a variety of surfaces [9–11]. Mussels affix themselves to various substrates, in particular wet surfaces, through specific adhesive protein molecules, commonly referred to as mussel adhesive proteins (MAPs), present in their byssal threads. Waite *et al.*, in the 1980s, first pioneered the study of these byssal proteins and identified the biochemistry behind mussel adhesion [12–14], focusing on the characterization of the byssal proteins present in the closest proximity to the adhering surface [15]. It is now well known that these proteins contain a high proportion of post-translationally modified amino acids, the most prominent being 3,4-dihydroxyphenylalanine (DOPA), formed through hydroxylation of tyrosine residues by a polyphenoloxidase enzyme [16]. The prominence of DOPA in MAPs suggests its importance in mussel bioadhesion [17]. In particular, DOPA molecules present in MAPs are able to form strong complexes with metal ions and metal oxides through coordination metal bridges [18,19]. Furthermore, the high degree of polyhydroxylated residues encountered in MAPs enables the formation of multiple hydrogen bonds [20]. Another remarkable property of DOPA is its structural simplicity: DOPA and its analogs are small and are therefore easily incorporated into materials destined for adhesion to a wide variety of substrates [21].

Mytilus edulis has been the most studied amongst the various species of mussels, and six major types of foot protein have been identified (*M. edulis* foot proteins, Mefp's, 1–6), each playing a spe-

* *Correspondence to: Conan J. Fee, Biomolecular Interaction Centre, University of Canterbury, Christchurch, New Zealand. E-mail: conan.fee@canterbury.ac.nz*

a *Department of Chemical and Process Engineering, University of Canterbury, Christchurch, New Zealand*

b *Biomolecular Interaction Centre, University of Canterbury, Christchurch, New Zealand*

c *Free Radical Biochemistry, School of Biological Sciences, University of Canterbury, Christchurch, New Zealand*

d *Department of Radiology, University of Otago Christchurch, New Zealand*

Journal of PeptideScience

cific role in the byssal thread [9]. Amongst these, Mefp-5, with a molecular weight (MW) of 9.5 kDa, lies closest to the substrate surface and is found to contain the highest DOPA content (~30%) [22].

In this study, we compared the adhesive properties of DOPA-containing peptides with those of the corresponding tyrosine-containing peptides. Two peptide sequences with high tyrosine content, inspired by the full protein sequence of Mefp-5, were synthesized. The wild-type Mefp-5 sequence contains DOPA residues, whereas the synthetic peptide fragments used in this study initially contained only tyrosine residues. These were subsequently chemo-enzymatically hydroxylated to DOPA using mushroom tyrosinase to resemble wild-type Mefp-5 peptide sequences. Adsorption of the unmodified and modified peptides on stainless steel surfaces was studied using a quartz crystal microbalance with dissipation (QCM-D) system, and the extent of adhesion was correlated to the conversion of tyrosine to DOPA.

Materials and Methods

Reagents

Peptides I and II (KGYKYYGGSS and KGYKYY, respectively) were ordered from Genscript (Piscataway, NJ, USA). These synthetic fragments contained tyrosine residues that could subsequently be modified chemo-enzymatically to DOPA. Trichloroacetic anhydride was obtained from Merck & Co., Inc. (NJ, USA). Argon and nitrogen gases were obtained from BOC gases (Christchurch, New Zealand). HPLC-grade acetonitrile was obtained from JT Baker®, Mallinckrodt Baker Inc. (PA, USA). Decon-90 was purchased from Agar Scientific (Chelmsford, United Kingdom). All other chemicals used in this work, including *L*-tyrosine, *L*-DOPA, mushroom tyrosinase (~2000 units/mg), mercaptoacetic acid, phenol, sodium carbonate salt, Trizma salt, and anhydrous trifluoroacetic acid (TFA), were obtained from Sigma Aldrich (St. Louis, MO, USA). All buffers were degassed prior to use.

Modification of Tyrosine to DOPA in Peptide Sequences

Tyrosine residues present in the peptide fragments were converted to DOPA by incubation with mushroom tyrosinase, following the methods previously described by Ito *et al.* [23] and Gieseg *et al.* [24]. Briefly, 100 nmol/ml of the peptide fragments were incubated with 200 units/ml of mushroom tyrosinase for 0 (control), 2, 4, and 6 h in a final volume of 1 ml of 100 mM sodium phosphate buffer pH 7.4 (one tyrosinase unit is defined as the amount of enzyme that produces a 0.001/min increase in absorbance at 280 nm in a 3 ml reaction mixture containing *L*-tyrosine at pH 6.5 and 25 °C). Reaction was quenched by denaturing the tyrosinase enzyme using 0.5 ml of 5% v/v trichloroacetic anhydride solution.

Separation of Unreacted Tyrosinase from Peptide Samples and Buffer Exchange

Through a 0.22-μm syringe filter (MS ® PES syringe filter, Membrane-Solutions, OH, USA), 500 μl of the reaction mixture were pre-filtered and injected onto a Sephadex™ Peptide SEC column 10/300 GL (GE Healthcare Technologies, Uppsala, Sweden) connected to an AKTAexplorer 10XT liquid chromatography system (Amersham Pharmacia Biotech, Uppsala, Sweden), using 10-mM Tris, pH 7.5 as running buffer at a flow rate of 0.25 ml/min. This procedure simultaneously enabled the following: (i) the separation of the modified peptide fragments from the mushroom tyrosinase enzyme and (ii) buffer exchange from the phosphate buffer used in the reaction step into Tris buffer. The peak containing the peptide fragments was collected, and its concentration was measured using a Nanodrop™ Spectrophotometer A280 nm (ThermoFisher Scientific, Waltham, MA, USA).

Hydrolysis of Peptide Sequences

Peptide hydrolysis was carried out on the DOPA-modified samples using acid vapor, following a protocol similar to the one previously described by Ito *et al.* [23] and Gieseg *et al.* [24]. In brief, 200 μl of the purified peptide fractions were placed in a 7.5 mm i.d. glass Durham tube and dried under vacuum overnight. The Durham tube containing the dried peptide sample was then placed into a Pico-Tag vial (Millipore, Bedford, MA, USA) containing 1 ml of 6 M HCl, 1% w/v phenol, and 50 μl mercaptoacetic acid. Argon was thoroughly flushed through the Pico-Tag vials for 5 min to remove oxygen; then the argon was extracted using a vacuum pump connected to a Speed Vac ® Plus AR system (Savant Instruments, Farmingdale, NY, USA) for 5 s, ensuring that the vacuum gauge pressure was below 200 mTorr. Acid hydrolysis was eventually carried out by incubating the vials in an oven at 110 °C for 24 h. The samples were then lyophilized using the Speed Vac system connected to a −110 °C freeze trap. The lyophilized samples were re-dissolved in 200 μl of 0.1% TFA, transferred to Eppendorf tubes, and centrifuged at 20 000 × g for 10 min. Twenty microliter of the supernatant was used for the identification and quantification of the hydrolyzed amino acid residues by HPLC as described later.

Quantification of DOPA and Tyrosine Residues in Peptide Hydrolysate

Analytical HPLC was carried out using a Shimadzu™ 10A instrument (Shimadzu Corporation, Kyoto, Japan) with 10 AD pumps, column oven, and RF-10AXL Shimazdu fluorescence detector Model-1050 (Shimadzu Corporation). The separation of the hydrolysed components was performed by gradient reverse phase HPLC using an Aqua™ C18 HPLC column, (250 × 4.6 mm ID, 5 μm column, Phenomenex, Auckland, New Zealand) run at 1 ml/min. Twenty microliter of the hydrolysate was injected, and the amino acid eluted using two subsequent linear gradients, the first from 1% acetonitrile in 0.1% TFA pH 2.5–15% acetonitrile in same TFA buffer in 14 min, followed by an increase to 50% acetonitrile in 2 min. The eluted DOPA and tyrosine were detected at their native fluorescence (excitation wavelength 280 nm/emission wavelength 320 nm). The hydrolyzed samples were analyzed in triplicate. The identities and concentrations of DOPA and tyrosine in the hydrolyzed samples were confirmed using pure samples as reference standards. The analysis of reference standards and samples resulted in highly repeatable peak areas with retention times varying within 5% between runs.

Adsorption of Peptide Sequences on Stainless Steel Surfaces

Cleaned stainless steel-coated quartz sensors were mounted in a Q-Sense E4 QCM-D system equipped with four measuring chambers (ATA Scientific, Tarren Point, New South Wales, Australia). The sensor crystals used in the experiments were coated with stainless steel grade 316, characterized by an isoelectric point of ~3–4. The detailed chemical composition of the metal surfaces, X-ray photon scattering survey reports, roughness data, and methods for deposition of the stainless steel coating on the sensor crystals were described in detail by Anand *et al.* [25]. The peptide solutions were

fed using a peristaltic pump (Ismatec IPC-N Pump, IDEX Health & Science, Wertheim, Germany) at a flow rate of 0.1 ml/min. The adsorption tests included an initial sensor equilibration step carried out with 10 mM Tris buffer, followed by an adsorption step, in which solutions containing the purified peptides at 1 mg/ml were fed to the system until stable frequency and dissipation signals were obtained. The sensors were then washed using Tris buffer, and removal/desorption of the protein from the surface was monitored until stable frequency and dissipation signals were obtained. The measurements were recorded using QSoft™ control software and further analyzed by applying the Sauerbrey model in QTools™ software (both programs supplied with the QCM-D instrument).

Cleaning of the sensors was performed as described in the study of Chandrasekaran *et al.* [26]. Briefly, at the end of each adsorption experiment, the sensor surface was cleaned with 1% Decon solution in MilliQ water. A second *ex situ* cleaning of the stainless steel sensors was performed between experiments using Pirhana solution [5 : 1 : 1 mixture of MilliQ water, ammonia (25%), and hydrogen peroxide (30%)], followed by a MilliQ water rinse. Sensors were then dried using nitrogen and UV irradiated for 10 min [26,27].

As described in the Results and Discussion section, the dissipation changes observed during the adsorption experiments were negligible. Therefore, the adsorbed layer was considered rigidly adsorbed on the stainless steel surface, and the amounts of peptide adsorbed were determined using the Sauerbrey model, in which the change in resonant frequency, Δf, is directly proportional to the mass accumulated on the surface, Δm, as follows [28]:

$$\Delta m = -\frac{\rho v \Delta f}{2 f_0 n} = -\frac{\rho t \Delta f}{f_0 n} = -C\frac{\Delta f}{n}, \quad (1)$$

where f_0 is the fundamental frequency when the sensor surface is clean; ρ, v, and t are the specific density, the shear wave velocity, and the thickness of the quartz sensor, respectively; and n is the overtone of the acoustic oscillation. For a 5-MHz quartz crystal, the constant C is equal to 17.7 ng/cm^2 Hz [29].

Results and Discussion

Mussel adhesive proteins are characterized by high DOPA content, which is considered to be the key in mussel adhesion and cohesion. In nature, post-translational modification of tyrosine to DOPA occurs at the highest levels in proteins located near the adhesion plaque–substratum interface. Amongst the six Mefp's contained in the mussel thread, Mefp-5 and Mefp-6 have been found in the region of the adhesive pad in contact with the substrate and are therefore considered to be mainly responsible for interfacial adhesion to surfaces [13,30,31]. In the present study, we considered two synthetic peptide fragments derived from the Mefp-5 regions with high DOPA content, namely, KGYKYYGGSS (Peptide I) containing 30% tyrosine and KGYKYY (Peptide II) containing 50% tyrosine. Both synthetic peptides initially contained three tyrosine residues, which were subsequently converted to DOPA through post-translational hydroxylation using mushroom tyrosinase. The specific influence of DOPA content on peptide adhesion was determined by partial conversion of the tyrosine residues. To this aim, the peptide fragments were incubated with mushroom tyrosinase for different times, i.e. 0, 2, 4, and 6 h. Zero-h samples, used as a negative control, were treated identically with the other samples. After the enzyme catalyzed reaction was quenched and the deactivated mushroom tyrosinase was removed, DOPA and tyrosine content in the purified peptides was determined by acid hydrolysis, followed by reversed-phase HPLC. In parallel experiments, surface adsorption of the peptides containing different levels of DOPA content/conversion was studied using QCM-D.

Conversion of Tyrosine to DOPA in Peptide Fragments

Figure 1 shows the reversed-phase chromatograms for hydrolyzed Peptide I after incubation with mushroom tyrosinase. Similar results were obtained for Peptide II. The chromatogram shows retention times from 4.5 to 7.5 min, during which period tyrosine and DOPA elute from the column. The control (0 h) sample showed a single large peak corresponding to tyrosine. However, HPLC analysis of the modified peptide fragments showed a peak at 5 min corresponding to the presence of DOPA in the sample. The area of the DOPA peak increased at 2, 4, and 6 h, with corresponding decreases in the peak areas corresponding to tyrosine. This result clearly demonstrates the increasing conversion of tyrosine to DOPA in the peptide fragments with time. The concentration of DOPA and tyrosine in the samples was determined from the area under the peaks by reference to the peak areas of DOPA and tyrosine standard solutions at known concentrations.

Fractional conversion of the tyrosine residues, χ, was defined as the amount of tyrosine consumed with respect to its initial amount:

$$x = \frac{c_{Tyr}^{in} - c_{Tyr}^{fin}}{c_{Tyr}^{in}}, \quad (2)$$

where c_{Tyr}^{in} and c_{Tyr}^{fin} are the initial and final concentrations of tyrosine in the peptide sample. Assuming the reaction from tyrosine to DOPA is stoichiometric (i.e. one molecule of DOPA is formed from one molecule of tyrosine) and no side reactions occur, then the amount of DOPA produced corresponds to the tyrosine residues consumed, $c_{Tyr}^{in} - c_{Tyr}^{fin} = c_{DOPA}^{fin}$; hence, the conversion can be rewritten as:

$$x = \frac{c_{DOPA}^{fin}}{c_{Tyr}^{in}}, \quad (3)$$

where c_{DOPA}^{fin} represents the final concentration of DOPA in the peptide samples after conversion by tyrosinase.

Figure 2 represents the decrease in concentration of tyrosine and corresponding increase in concentration of DOPA at 2, 4, and 6 h of incubation with tyrosinase enzyme. Note that the concentration

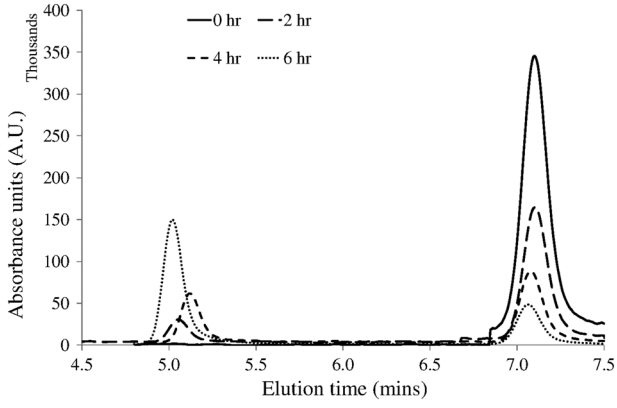

Figure 1. High performance liquid chromatography chromatograms of hydrolyzed Peptide I fragment incubated with mushroom tyrosinase for 0, 2, 4, and 6 h. The peaks at retention times of ~5 and 7.1 min correspond to 3,4-dihydroxyphenylalanine and *L*-tyrosine, respectively, as determined using pure standards for the two amino acids.

Journal of PeptideScience

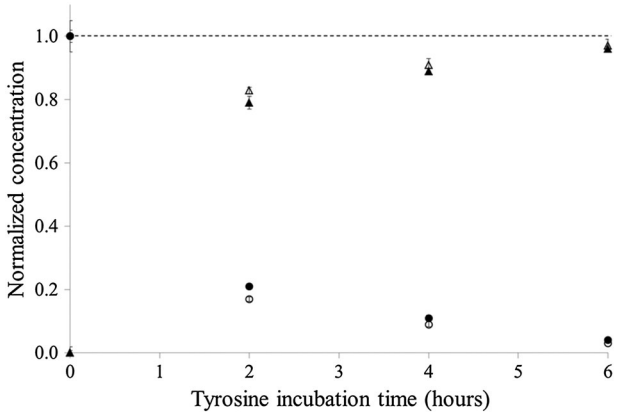

Figure 2. Concentration of tyrosine (circles) and 3,4-dihydroxyphenylalanine (triangles) for Peptide I (full symbols) and Peptide II (empty symbols) at 0, 2, 4, and 6 h of incubation with mushroom tyrosinase. Data were normalized against initial concentration of tyrosine residues. Note that data for DOPA correspond to fractional conversion.

data are normalized against the initial concentration of tyrosine present in the samples; hence, the normalized concentration for DOPA also corresponds to the conversion previously defined. After 2 h of incubation with mushroom tyrosinase, conversion was in the order of 80% for both peptides, indicating that, on average, at least two of the three tyrosine residues present in the peptide backbones had been converted to DOPA by this time. Conversion steadily increased with time, and after 6 h of incubation with the enzyme, both peptides showed conversions in the range ~97–99%, indicating that virtually, all of the tyrosine in the peptide sample was converted to DOPA in the time range investigated. After 2 h incubation, conversion is slightly higher for Peptide II than for Peptide I, but this difference is practically lost after 4-h incubation. For this reason, it is safe to conclude that the conversion kinetics is similar for the two peptides.

Surface Adsorption of Modified Peptides Using QCM-D

The main objective of this study was to compare the adsorption of modified with unmodified peptide fragments on a stainless steel surface. Note that two separate and independent control experiments were performed, one with peptides as received (no incubation in mushroom tyrosinase) and a second one with peptides incubated for 0 h in mushroom tyrosinase. The adsorption results were comparable, reflecting the negligible conversion of tyrosine to DOPA in the 0-h control, as also presented in the previous section. For this reason, only adsorption results for the 0-h incubated peptides will be presented in the following.

Quartz crystal microbalance with dissipation measures simultaneous changes in resonance frequency (f) and dissipation (D) caused by adsorption on the sensor surface. Changes in frequency correspond to variations in the mass adsorbed, while changes in dissipation relate to modifications in the viscoelastic properties (shear, viscosity, and density) of the adsorbed layer. An indication of whether the adsorbed layer is rigid or viscoelastic can be attained through an evaluation of the dimensional ratio $\Delta D/(-\Delta f/n)$, i.e. the slope of a ΔD *versus* Δf plot. As a rule of thumb, for a 5-MHz sensor, if the dissipation shift observed with respect to the frequency change is small ($\Delta D/(-\Delta f/n) < 4\times10^{-7}$ Hz^{-1}), then viscoelastic dissipation of energy can be neglected, and the Sauerbrey model can be used to interpret QCM-D data [28,32–34]. For all experiments, the dimensional ratio fell in the range 1.5–2.2 $\times 10^{-7}$ Hz^{-1}; hence, it is reasonable to consider that the adsorbed layers were rigidly coupled to the sensor surface, consistent with the formation of a thin layer composed of the small peptide molecules. Figure 3 shows the mass of peptide adsorbed per unit surface area, q, for the modified and unmodified peptide samples.

The adsorption results reveal that unmodified peptides are able to adsorb onto the stainless steel surface creating a layer in the order of 2 mg/m^2. This result is not surprising as adsorption of peptide fragments and proteins on stainless steel is a known phenomenon, mostly associated to the formation of a fouling layer deleterious to process equipment [26]. Adsorption of the investigated peptides can be mediated through electrostatic bonds between the polar lysine residues to the charged stainless steel surface, as well as the interactions between the π-electrons of the aromatic ring present in the tyrosine residues [35].

Surface adsorption progressively increased with the incubation times between peptides and mushroom tyrosinase. In particular, compared with the native peptide control samples, the adsorption of the 2-h modified samples showed an approximately twofold increase; 4-h modified samples showed a 2.5-fold increase; and the 6-h modified samples showed a fivefold increase. The higher amount of adsorbed peptides following modification with respect to the control is uniquely due to the presence of DOPA. The enhanced propensity for adsorption of DOPA-containing peptides can be primarily associated with the interaction of the catechol moieties. The two hydroxyl groups on the benzene ring of DOPA are able to form strong metal ion chelate complexes, linking the DOPA molecule with metal surfaces [36–38]. Also, catechol groups are capable of being both hydrogen donor and acceptor, hence allowing DOPA molecules to compete with water for hydrogen bonding sites on hydrophilic surfaces such as stainless steel [35]. It is also plausible that the difference in adsorption observed is related to different orientations and conformations of the adsorbed peptides. In fact, adsorbed aromatic amino acids orient parallel to metal surfaces [39], while DOPA molecules interact with surfaces in an 'upright' position thanks to the formation of bidentate complexes between the two hydroxyl groups and surface metal ions [40,41]. Such difference allows a higher surface concentration of the modified peptides with respect to unmodified tyrosine-containing peptides. Finally, the higher amount of adsorption for the modified peptides can be partly explained by the tendency of DOPA to self-aggregate and cross-link through quinone and eumelanin formation [36,42–44].

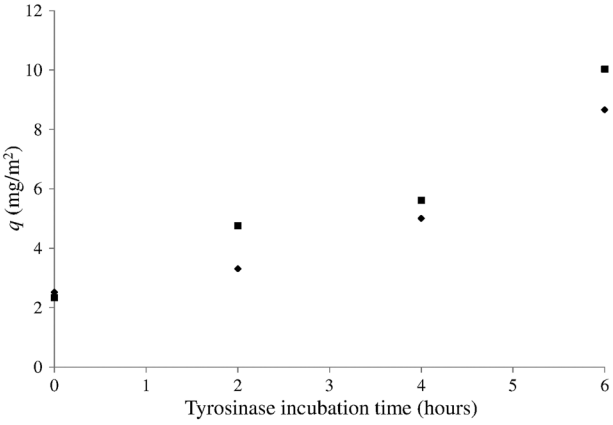

Figure 3. Adsorption of unmodified (0-h control) peptide fragments and those modified under different tyrosinase incubation times on stainless steel surfaces. Peptide I (diamonds) and Peptide II (squares).

Similar considerations can be reasonably extended to longer amino acidic sequences including large proteins such as Mefp's, even though in this case, statistical and entropic factors will also contribute to further enhance surface adsorption [45]. Future work is planned with additional peptides of similar molecular weights but containing different amounts of DOPA residues, as well as adsorption experiments with natural and recombinant Mefp's. Results of these experiments will help separate the different contributing factors to adsorption of DOPA containing sequences.

From the data presented in Figure 3, it appears that Peptide II has a greater propensity to interact with and adsorb on the stainless steel substrate than Peptide I. This difference is even more pronounced if the amount adsorbed is plotted in molar terms as Peptide I (ten amino acid residues, MW 1.1 kDa) is larger than Peptide II (six amino acid residues, MW 0.8 kDa). This observation can be derived, amongst others, from the following: (i) differences in the global amino acid sequence of the two peptides, (ii) differences in the amino acid residues other than tyrosine/DOPA, and (iii) differences in the location/s of the tyrosine residues converted to DOPA. Peptide I is extremely similar to Peptide II but in the four amino acids at the C-terminus, namely, two glycine followed by two serine residues. The steric effect associated to these additional residues likely hinders the surface interactions of the two vicinal DOPA molecules, which are instead positioned at the C-terminus in Peptide II and with higher ability to adsorb to the stainless steel substrate. Also, it is reasonable to suppose that Peptide I has a smaller adsorption energy than Peptide II, mainly due to the additional nonpolar glycine residues that display relatively low affinity towards the charged and polar metal oxides ubiquitously present on the stainless steel surface [25]. Finally, the differences in the peptide sequence might also affect the action of the mushroom tyrosinase enzyme and the location of the tyrosine residues hydroxylated to DOPA, hence the adsorption behavior of the two peptides.

Conclusions

In this study, the influence of DOPA residues on peptide adhesion onto stainless steel surfaces was studied. Two peptide fragments inspired from Mefp-5, KGYKYYGGSS and KGYKYY, were studied because of their high relative tyrosine contents. Tyrosine residues in the peptide fragments were enzymatically converted to DOPA by mushroom tyrosinase. The degree of the conversion increased with tyrosinase incubation time, with almost complete conversion of the tyrosine residues to DOPA after 6 h.

Adsorption of the native and modified peptides on stainless steel surfaces were carried out by QCM-D, demonstrating a strong correlation between the degree of DOPA conversion and surface adsorption. Maximum adsorption was observed with the peptides incubated for 6 h. At this time, almost complete conversion of tyrosine to DOPA was associated with a fourfold increase in surface adsorption compared with the unmodified peptides containing only tyrosine residues.

Comparable results were obtained with the two peptides fragments studied, suggesting that similar results might be expected with other DOPA-containing peptides and, by extension, polypeptides, e.g. proteins containing the catechol side chain.

This study offers an approach to the manufacture of adhesive polypeptides, starting from tyrosine-containing peptide sequences, by using tyrosine hydroxylases enzymes to convert tyrosine residues to DOPA residues. Future work will focus on the extension of this preparation protocol to other sequences and the use of modified peptides to create antifouling agents for stainless steel by coupling the adhesive peptide sequence to an antifouling agent as polyethylene glycol.

Acknowledgement

N. Chandrasekaran is grateful to the University of Canterbury for a UC Doctoral Scholarship.

References

1 Dimartino S, Lir I, Haber M, Azhari R. Characterization of biomimetic adhesives from the red alga *Gracilaria Conferta* for biomedical applications. In *Biological and Biomimetic Adhesives: Challenges and Opportunities*, Flammang P, Santos R, Aldred N, Gorb S (eds). The Royal Society of Chemistry: Cambridge, 2013; 117–131.
2 Keckes J, Burgert I, Frühmann K, Müller M, Kölln K, Hamilton M, Burghammer M, Roth SV, Stanzl-Tschegg S, Fratzl P. Cell-wall recovery after irreversible deformation of wood. *Nat. Mater.* 2003; **2**: 810–814.
3 Schreiber L, Franke R, Hartmann K. Wax and suberin development of native and wound periderm of potato (*Solanum tuberosum L.*) and its relation to peridermal transpiration. *Planta* 2005; **220**: 520–530.
4 Flammang P, Adhesive secretions in echinoderms: an overview. In *Biological Adhesives*, Smith AM, Callow JA (eds). Springer Berlin: Heidelberg, 2006; 183–206.
5 Voigt D, Gorb S. An insect trap as habitat: cohesion-failure mechanism prevents adhesion of *Pameridea roridulae* bugs to the sticky surface of the plant *Roridula gorgonias*. *J. Exp. Biol.* 2008; **211**: 2647–2657.
6 Creton C, Papon E. Materials science of adhesives: how to bond things together. *MRS Bull.* 2003; **28**: 419–423.
7 Rischka K, Richter K, Hartwig A, Kozielec M, Slenzka K, Sader R, Grunwald I. Bio-inspired polyphenolic adhesives for medical and technical applications. In *Biological Adhesive Systems*, Byern J, Grunwald I (eds). Springer: Vienna, 2010, pp 201–211.
8 Silverman HG, Roberto FF. Understanding marine mussel adhesion. *Mar. Biotechnol.* 2007; **9**: 661–681.
9 Bandara N, Zeng H, Wu J. Marine mussel adhesion: biochemistry, mechanisms, and biomimetics. *J. Adhes. Sci. Technol.* 2013; **18-19**: 2139–2162.
10 Deming TJ. Mussel byssus and biomolecular materials. *Curr. Opin. Chem. Biol.* 1999; **3**: 100–105.
11 Hwang DS, Zeng H, Masic A, Harrington MJ, Israelachvili JN, Waite JH. Protein-and metal-dependent interactions of a prominent protein in mussel adhesive plaques. *J. Biol. Chem.* 2010; **285**: 25850–25858.
12 Waite JH. Determination of (catecholato)borate complexes using difference spectrophotometry. *Anal. Chem.* 1984; **56**: 1935–1939.
13 Waite JH, Andersen NH, Jewhurst S, Sun C. Mussel adhesion: finding the tricks worth mimicking. *J. adhesion* 2005; **81**: 297–317.
14 Waite JH. The phylogeny and chemical diversity of quinone-tanned glues and varnishes. *Comp. Biochem. Physiol. B* 1990; **97**: 19–29.
15 Bi RC, Dauter Z, Dodson E, Dodson G, Giordano F, Reynolds C. Insulin's structure as a modified and monomeric molecule. *Biopol.* 1984; **23**: 391–395.
16 Silverman HG, Roberto FF. Understanding marine mussel adhesion. *Mar. Biotechnol.* 2007; **9**: 661–681.
17 Lee BP, Messersmith P, Israelachvili J, Waite JH. Mussel-inspired adhesives and coatings. *Ann. Rev. Mater. Res.* 2011; **41**: 99–132.
18 Baty AM, Leavitt PK, Siedlecki CA, Tyler BJ, Suci PA, Marchan RE, Geesey GG. Adsorption of adhesive proteins from the marine mussel, *Mytilus edulis*, on polymer films in the hydrated state using angle dependent XPS and AFM. *Langmuir* 1997; **13**: 5702–5710.
19 Wilke P. Börner HG, Mussel-glue derived peptide-polymer conjugates to realize enzyme-activated antifouling coatings. *ACS Macro Lett.* 2012; **1**: 871–875.
20 Waite JH, Qin X. Polyphosphoprotein from the adhesive pads of Mytilus edulis. *Biochem.* 2001; **40**: 2887–2893.
21 Brubaker CE, Messersmith PB. The present and future of biologically inspired adhesive interfaces and materials. *Langmuir* 2012; **28**: 2200–2205.
22 Marumo K, Waite J. Optimization of hydroxylation of tyrosine and tyrosine-containing peptides by mushroom tyrosinase. *Biochim. Biophys. Acta* 1986; **872**: 98–103.

23 Ito S, Kato T, Shinpo K, Fujita K. Oxidation of tyrosine residues in proteins by tyrosinase. Formation of protein-bonded 3,4-dihydroxyphenylalanine and 5-S-cysteinyl-3,4-dihydroxyphenylalanine. *Biochem. J.* 1984; **222**: 407–411.
24 Gieseg SP, Simpson JA, Sharlton TS, Duncan MW, Dean RT. Protein-bound 3,4-dihydroxyphenylalanyne is a major reductant formed during hydroxyl radical damage to proteins. *Biochem.* 1993; **32**: 4780–4786.
25 Anand G, Zhang F, Linhardt RJ, Belfort G. Protein-associated water and secondary structure effect removal of blood proteins from metallic substrates. *Langmuir* 2010; **27**: 1830–1836.
26 Chandrasekaran N, Dimartino S, Fee CJ. Study of the adsorption of proteins on stainless steel surfaces using QCM-D. *Chem. Eng. Res. Des.* 2013; **91**: 1674–1683.
27 Chandrasekaran N, Dimartino S, Fee CJ. Adsorption of proteins on stainless steel surfaces.In *Proceedings of Chemeca Conference*, Wellington: New Zealand, 2012; 23–26.
28 Sauerbrey G. The use of quartz crystals for weighing thin layers and for microweighing. *J. Geophys. Res.* 1959; **155**: 206–222.
29 Malmström J, Agheli H, Kingshott P, Sutherland DS. Viscoelastic modeling of highly hydrated laminin layers at homogeneous and nanostructured surfaces: quantification of protein layer properties using QCM-D and SPR. *Langmuir* 2007; **23**: 9760–9768.
30 Benedict CV, Picciano PT. Adhesives from marine mussels. In *Adhesives from Renewable Resources*, ACS Symposium Series, Vol. **385**, Hemingway RW, Conner AH, Branham SJ (eds). American Chemical Society: Washington, 1989; 465–483.
31 Lee H, Scherer NF, Messersmith PB. Single-molecule mechanics of mussel adhesion. *Proc. Natl. Acad. Sci. U. S. A.* 2006; **103**: 12999–13003.
32 Irwin EF, Ho JE, Kane SR, Healy KE. Analysis of interpenetrating polymer networks via quartz crystal microbalance with dissipation monitoring. *Langmuir* 2005; **21**: 5529–5536.
33 Stengel G, Höök F, Knoll W. Viscoelastic modeling of template-directed DNA synthesis. *Anal. Chem.* 2005; **77**: 3709–3714.
34 Reviakine I, Johannsmann D, Richter RP. Hearing what you cannot see and visualizing what you hear: interpreting quartz crystal microbalance data from solvated interfaces. *Anal. Chem.* 2011; **83**: 8838–8848.
35 Sever MJ, Weisser JT, Monahan J, Srinivasan S, Wilker JJ. Metal-mediated cross-linking in the generation of a marine-mussel adhesive. *Angew. Chem.* 2003; **116**: 454–456.
36 Fant C, Hedlund J, Höök F, Berglin M, Fridell E, Elwing H. Investigation of adsorption and cross-linking of a mussel adhesive protein using Attenuated Total Internal Reflection Fourier Transform Infrared Spectroscopy (ATR-FTIR). *J. Adhes.* 2010; **86**: 25–38.
37 Monahan J, Wilker JJ. Specificity of metal ion cross-linking in marine mussel adhesives. *Chem. Commun.* 2003; **14**: 1672–1673.
38 Lee B, Dalsin J, Messersmith P. Biomimetic adhesive polymers based on mussel adhesive proteins In *Biological Adhesives*, Smith AM, Callow JA (eds). Springer Berlin: Heidelberg, 2006; 257–278.
39 Arwin H, Lundstrom I, Arielly S, Claeson G. Orientation of a tripeptide on platinum. *Langmuir* 1990; **6**: 1551–1557.
40 Olivieri M, Baier RE, Loomis RE. Surface properties of mussel adhesive protein component films. *Biomaterials* 1992; **13**: 1000–1008.
41 Gao Z, Bremmer P, Barker MF, Wui Tan E, McQuillan AJ. Adhesive secretions of live mussels observed in situ by attenuated total reflection-infrared spectroscopy. *Appl. Spectroscopy* 2007; **61**: 55–59.
42 Waite JH. The phylogeny and chemical diversity of quinone-tagged glues and varnishes. *Comp. Biochem. Physiol. B* 1990; **97**: 19–29.
43 Fant C, Sott K, Elwing H, Hook F. Adsorption behavior and enzymatically or chemically induced cross-linking of a mussel adhesive protein. *Biofouling* 2000; **16**: 119–132.
44 Hwang DS, Yoo HJ, Jun JH, Moon WK, Cha HJ. Expression of functional recombinant mussel adhesive protein Mgfp-5 in Escherichia coli. *Appl. Environ. Microb.* 2004; **70**: 3352–3359.
45 Stewart RJ, Ransom TC, Hlady V. Natural underwater adhesives. *J. Polym. Sci. Pol. Phys.* 2011; **49**: 757–771.

